Journal of Geodynamics 111 (2017) 31–42

Contents lists available at ScienceDirect

Journal of Geodynamics

journal homepage: www.elsevier.com/locate/jog

# Late Cretaceous to Cenozoic deformation and exhumation of the Chilean Frontal Cordillera (28°–29°S), Central Andes

Fernando Martínez[a,*], Mauricio Parra[b], César Arriagada[c], Andrés Mora[d], Sebastián Bascuñan[c], Matías Peña[c]

[a] Departamento de Ciencias Geológicas, Facultad de Ingeniería, Universidad Católica del Norte, Angamos 0610, Antofagasta, Chile
[b] Institute of Energy and Environment, University of Sao Paulo, Sao Paulo, Brazil
[c] Departamento de Geología, FCFM, Universidad de Chile, Chile
[d] Ecopetrol S.A. – Instituto Colombiano del Petróleo, Piedecuesta, Colombia

ARTICLE INFO

*Keywords:*
Frontal Chilean Cordillera
Incaic deformation
Tectonic inversion
Basement-involved deformation

ABSTRACT

The Frontal Cordillera in northern Chile is located over the flat-slab subduction segment of the Central Andes. This tectonic province is characterized by a thick-skinned structural style showing evidence of tectonic inversion and basement-involved compressive structures. Field data, U-Pb geochronological and apatite fission track data were used to unravel partially the tectonic history of the area. Previous U-Pb ages of synorogenic deposits exposed on the flanks of basement-core anticlines indicate that Andean deformation started probably during Late Cretaceous with the tectonic inversion of Triassic and Jurassic half-grabens. New U-Pb ages of the synorogenic Quebrada Seca Formation suggest that this deformation continued during Paleocene (66-60 Ma) with the reverse faulting of pre-rift basement blocks. The analysis of new apatite fission-track data shows that a rapid and coeval cooling related to exhumation of the pre-rift basement blocks occurred during Eocene times. This exhumation event is interpreted for first time in the Chilean Frontal Cordillera and it could have occurred simultaneously with the propagation of basement-involved structures. The age of this exhumation event coincides with the Incaic orogenic phase, which is interpreted as the most important to the Central Andes in terms of shortening, uplift and exhumation.

## 1. Introduction

The Central Andes of northern Chile between 27° and 28°S (Fig. 1) are located over the so-called “Pampean” flat-slab subduction segment defined originally by Baraganzi and Isacks (1976), which is mainly characterized by a volcanic gap on the Chilean side, as well as by the occurrence of a mixed thick- and thin-skinned deformation style (Jordan et al., 1983; Moscoso and Mpodozis, 1988; Mpodozis and Kay, 1990; Ramos et al., 2002; Martínez et al., 2016, among others). Here, the deformed belt is divided into two large, NNE-oriented tectonic provinces: the Coastal Cordillera and the Frontal Cordillera (Fig. 1). The tectonic evolution of both provinces was marked by a series of geological processes that include extensional deformation creating back-arc basins during Mesozoic times (Triassic-Jurassic; Mpodozis and Ramos, 2008), and compressional tectonic episodes and magmatism, which created thrust systems that led to shortening and thickening of the continental margin during the Cenozoic (Mpodozis and Ramos, 1989; Ramos et al., 2002; Ramos, 2009). Both tectonic processes (extension and compression) are mostly associated with the westward South America plate motion, changes in the convergence rate between the oceanic pacific plate and South America, as well as by the coupling between both plates (Moscoso and Mpodozis, 1988; Mpodozis and Ramos, 1989; Ramos et al., 2002; Ramos, 2010; Ramos and Folguera, 2009).

The Chilean Frontal Cordillera (Figs. 1 and 2) consists of a series of large (≥50 km-long) Permo-Triassic crystalline basement blocks, that are well-exposed along an extensive belt that forms part of a group of Upper Paleozoic to Low Mesozoic intrusives, similar to those the form the Cordillera Real in Ecuador and the Cordillera Real of Bolivia (Mpodozis and Ramos, 1989; Mpodozis and Kay, 1990; Gregori et al., 2003; Chew et al., 2007; Hervé et al., 2014). In northern Chile (Fig. 2), these basement blocks lie intercalated with NNE-striking belts made of Mesozoic and Cenozoic volcanic and sedimentary successions (Fig. 2) that record the successive episodes of deformation within this Andean segment (Jensen, 1976; Moscoso and Mpodozis, 1988; Moscoso et al., 2010; nez et al., 2015, 2016; nez et al., 2015, 2016). The present-day

* Corresponding author.
*E-mail address:* martinezfjh@hotmail.com (F. Martínez).

http://dx.doi.org/10.1016/j.jog.2017.08.004
Received 24 April 2017; Received in revised form 21 August 2017; Accepted 22 August 2017
Available online 08 September 2017
0264-3707/ 

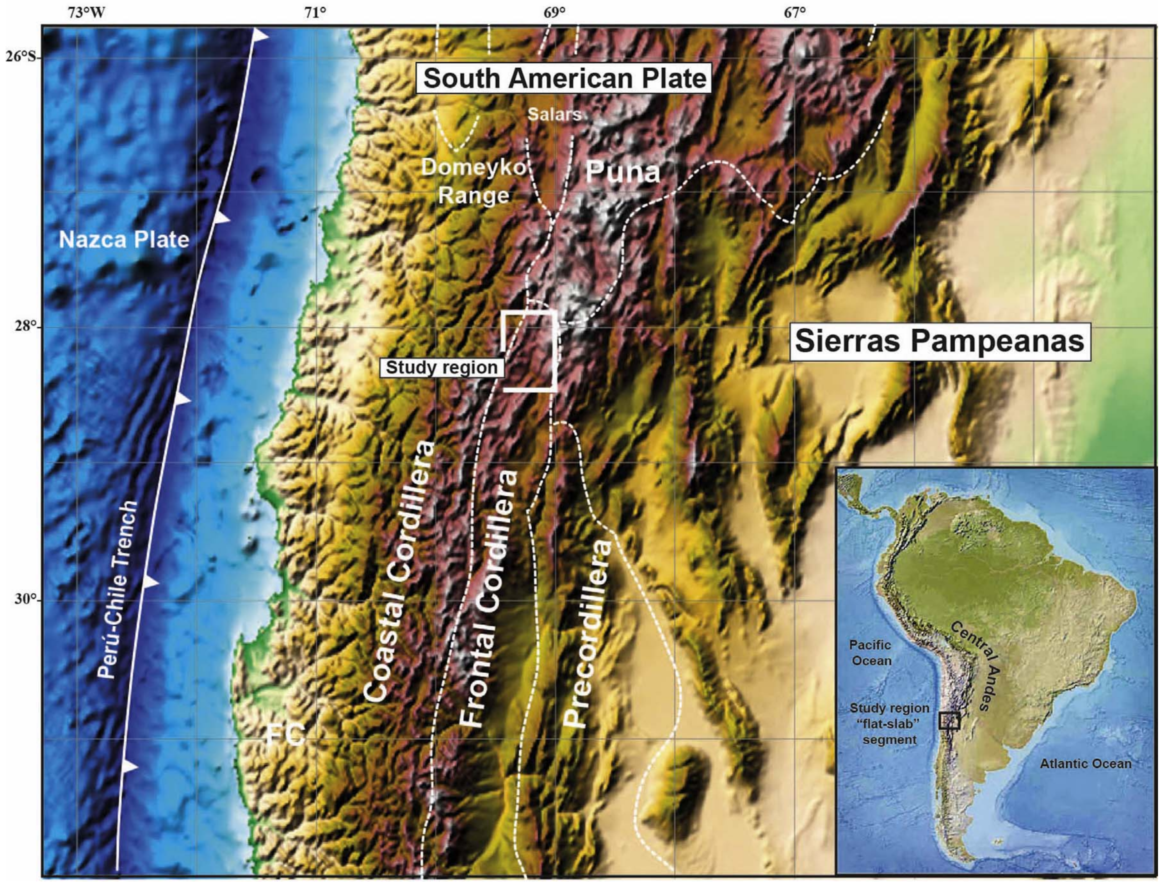


**Fig. 1.** Digital elevation model showing the distribution of the main tectonic provinces along the flat-slab subduction segment and the location of the study area.

architecture of the Frontal Cordillera has been usually compared with the structure of the Sierras Pampeanas in Argentina, which is dominated by basement-involved structures (Fig. 1). The genesis of these structures is related to the regional and horizontal compression of the continental margin caused by the shallowing of the Nazca plate under South America during the Cenozoic (Godoy and Davidson, 1974; Jordan et al., 1983; Moscoso and Mpodozis, 1988; Gutscher et al., 2000; Ramos et al., 2002; Cristallini et al., 2004; Martínez et al., 2016). However; recent studies (Peña et al., 2013; Martínez et al., 2012,2015) have interpreted specific structural styles (e.g., inversion structures), and new ages of deformation that suggest a tectonic scenario more complex than those proposed previously for this region (Moscoso and Mpodozis, 1988; Jordan et al., 1983; Ramos et al., 2002; Moscoso et al., 2010). They have interpreted the structure of the Frontal Cordillera as a result of tectonic inversion and thrusting of former Mesozoic extensional basins, mainly during Late Cretaceous and Paleocene times (Martínez et al., 2012, 2015; Peña et al.,2013). These results show that the Late Cretaceous to Cenozoic deformation of the Chilean Frontal Cordillera is not as simple as it was believed some years ago (Godoy and Davidson, 1974; Moscoso and Mpodozis, 1988).

Despite all the advances in the knowledge of the tectonic evolution of the Chilean Frontal Cordillera, the oldest deformation ages, as well as the exhumation history of their basement blocks is still an aspect to resolve. This problem is due to the fact that its tectonic history has mainly been constrained by some U-Pb and/or K-Ar ages from Oligocene and Miocene volcanic and sedimentary synorogenic deposits exposed in the easternmost part of this region, which only has allowed interpreting the younger episodes of contractional deformation. Recent studies (Peña et al., 2013; Martínez et al., 2015; Rossel et al., 2016) also point out that the Andean deformation in this region is not a response to a unique mechanism of crustal shortening (thrusting, tectonic inversion, among others) and different deformation styles appear to be superimposed. To know the timing of deformation and exhumation in this region, we provide new results of apatite fission track analysis from crystalline basement rocks of the Frontal Cordillera at this latitudes, which are combined with new U-Pb dating of the Cenozoic synorogenic deposits exposed on the footwalls of the basement thrusts. These data will allow obtaining an approximate scheme of the tectonic evolution of this part of the western Central Andes.

## 2. Background

### 2.1. Geological setting

The oldest rocks in the Frontal Cordillera in northern Chile between 27°–28°S consist of NNE-SSW trending Permo-Triassic granitic rocks (~245–250 Ma; Jensen, 1976; Mpodozis and Kay, 1990) and rhyolitic deposits (263–228 Ma; Thiele, 1964; Moscoso et al., 2010; Martínez et al., 2014). The granitic rocks have been grouped into the "Montosa Plutonic Complex" and the "Chollay Plutonic Complex" (Farrar et al., 1970; Jensen, 1976; Mpodozis and Kay, 1990; Martínez et al., 2014), which have been associated with subduction-related magmatism and post-subduction magmatic events that occurred along the continental margin during the final configuration of the Gondwana supercontinent (Mpodozis and Kay, 1990; Mpodozis and Kay, 1992; Hervé et al., 2014).

In the study area, from west to east, the granitic rocks are: the La Estancilla Granite, the Montosa Granite, the El Colorado Granite and the Chollay Granite (Fig. 2; Moscoso et al., 2010; Martínez et al., 2014). The rhyolitic deposits correspond to the Pastos Blanco Formation (Thiele, 1964; Moscoso et al., 2010) (Fig. 2 and 3). Previous works related the granitic rocks with the pre-rift basement of ancient extensional basins established in this region during the Mesozoic (Jensen,

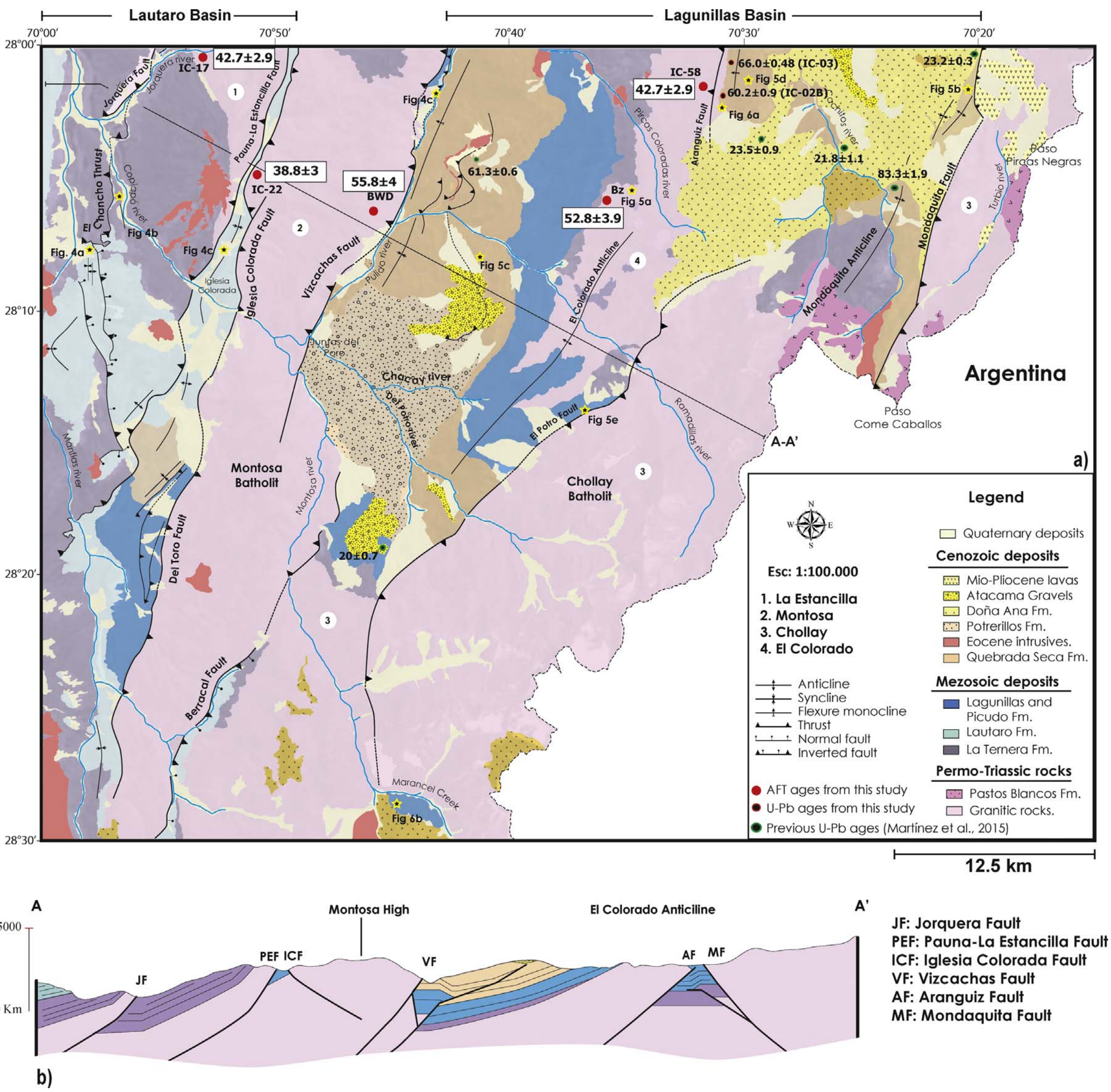


**Fig. 2.** (a) Geological map of northern Chile between 28°–28°30′S, showing the different structural styles and stratigraphic units exposed along the area (Modified from Martínez et al., 2015), (b) Geological cross section showing the structural style of the main structures indicated in the map. Note: black and yellow stars in the map indicate the location of the photos showed in the next Figs. 1: La Estancilla Granite, 2: Montosa Granite, 3: El Colorado Granite, 4: Chollay Granite. (For interpretation of the references to colour in this figure legend, the reader is referred to the web version of this article.)

1976; Mosocoso and Mpodozis, 1988; Mpodozis and Allmendinger, 1993; Mpodozis and Ramos, 2008; Martínez et al., 2012). These rocks form part of large basement blocks that are limited by NNE-striking reverse faults that separate them from Mesozoic and Cenozoic volcanic and sedimentary deposits. The latter deposits are related to the infill of the Lautaro and Lagunillas basins (Fig. 2), which correspond to Jurassic extensional back-arc basins (Jensen, 1976; Mpodozis and Ramos, 2008; Martínez et al., 2012; Oliveros et al., 2013), created during the fragmentation of western Gondwana.

Along the westernmost parts of the study area, in the Lautaro Basin (Fig. 2), the oldest Mesozoic deposits consist of thick (~2000 m) Upper Triassic continental volcanic and sedimentary *syn*-rift successions composed of interbedded red conglomerates, sandstones and basaltic andesites of the La Ternera Formation (Jensen, 1976; Charrier, 1979, among others) (Figs. 2 and 3), which unconformably overlie the Permo-Triassic granitic basement blocks (Fig. 2). Towards the western part of the basin, this formation is unconformably overlain by ~3000 m of Lower Jurassic syn-rift deposits composed of sedimentary continental and marine successions (limestones, calcareous sandstones and shales with marine fossils) defined as the Lautaro Formation (Jensen, 1976; Arévalo, 2005), which show rapid and dramatic thickness changes both across and along strike, suggesting a structural control, such as normal faulting. The Lautaro Formation is partially covered by 800 m of Tithonian-Kimmeridgian strata (Picudo Formation), interpreted as a post-rift sequence (Figs. 2 and 3) (Jensen, 1976; Oliveros et al., 2012; Martínez et al., 2015).

In the Lagunillas Basin (Fig. 2), the Mesozoic rocks correspond to 300 m of Upper Triassic syn-rift successions of the La Ternera Formation, which unconformably overlie the granitic rocks (Fig. 2). This formation is followed by 1200 m of Upper Jurassic continental syn-rift deposits of the Lagunillas Formation (Jensen, 1976; Oliveros et al., 2013), which is mainly composed of red sandstone, conglomerates and andesitic lavas (Fig. 2 and 3), cut by minor normal faults. Upwards, this unit is partly covered by a succession of Upper Jurassic clastic and volcanic rocks interpreted as a lateral equivalent of the Picudo Formation (Fig. 3).

Upper Cretaceous and Cenozoic deposits in the area include around 3000 m of continental successions that lie well-exposed along the western and eastern sectors of the Lagunillas Basin (Fig. 2), unconformably covering the Triassic and Jurassic syn-rift successions.

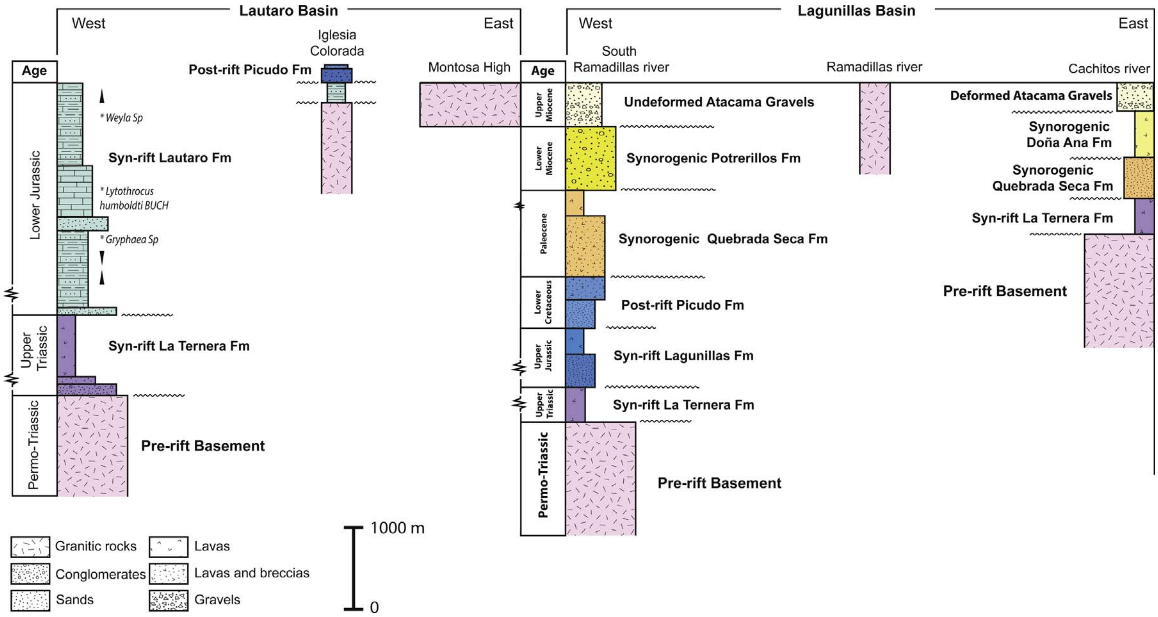


**Fig. 3.** Generalized stratigraphic columns of the geological units exposed along the Lautaro and Lagunillas basins in the Chilean Frontal Cordillera (27°–28°S). See locations of the columns in the geological map (Modified from Martínez et al., 2015).

These correspond to volcanic and sedimentary successions accumulated under a compressional setting (Godoy and Davidson, 1976; Jensen, 1976; Moscoso and Mpodozis, 1988; Moscoso et al., 2010; Martínez et al., 2015) composed of a basal section of approximately 1000 m of Upper Cretaceous-Paleocene synorogenic deposits comprised of interbedded red conglomerates, sandstones, breccias and tuffs with internal growth strata, defined as the Quebrada Seca Formation (Muzzio, 1980; Iriarte et al., 1999; Moscoso et al., 2010; Martínez et al., 2014). In the western sector of the Lagunillas Basin, these deposits are unconformably overlain by Oligo-Miocene conglomerates of the Potrerillos Formation (Reutter, 1974), while in the easternmost parts they are unconformably overlain by Lower Miocene andesitic and basaltic lavas of the Doña Ana Formation (Thiele, 1964). The Cenozoic deposits are capped by the Mid-Miocene, semi-consolidated sediments collectively called the Atacama Gravels, and Mio-Pliocene andesites found near the Chile-Argentina border (Fig. 2) (Jensen, 1976; Iriarte et al., 1999; Arévalo, 2005).

### 2.2. Structure of the Chilean Frontal Cordillera

The structure of this tectonic province is mainly dominated by an array of NNE-striking basement-involved compressive structures that include reverse faults, thrusts, basement-cored anticlines, inverted structures and other minor thin-skinned folds and thrusts (Fig. 2). Along the study area, the main structures correspond to a series of large basement blocks that have compartmentalized the architecture of the Lautaro and Lagunillas basins (Fig. 2a), which frequently are bounded by west and east-verging thrusts forming pop-up structures (e.g., Montosa Batolith), or thick-skinned triangle zones (Zapata and Allmendinger, 1996; Fig. 2 and 4 c ).

In the Lautaro Basin, the basement-involved structures consist of a series of thrust faults (Jorquera, Pauna-La Estancilla and Iglesia Colorada-Del Toro Fault Systems) (Godoy and Davidson, 1976; Jensen, 1976; Martínez et al., 2014) that modified the previous extensional tectonic configuration of the basin (Fig. 2)(Martínez et al., 2012). These correspond to double-verging (east and west) structures dipping approximately 30–50° at the surface, along which granitic blocks of pre-rift basement are placed over continental and marine Mesozoic (Triassic and Jurassic) syn-rift deposits (Fig. 4c), forming footwall syncline structures. In the central section of the basin, NNE-trending inverted structures have also been recognized, consisting of partially reactivated normal faults and west-verging asymmetrical folds related to inversion anticlines (Fig. 4a). The latter generally involve the Triassic and Jurassic syn-rift deposits, which show drastic lateral and vertical thickness changes, displaying wedge geometries (Fig. 4a). Here, other minor, east-verging, thin-skinned thrusts (El Chancho Thrust; Fig. 2 and 4b) have also been identified, but they are frequently linked to subsidiary structures that accommodated horizontal displacement of major basement-involved compressive structures.

In the Lagunillas Basin, the main structures correspond to NNE-striking thrust faults, basement-cored anticlines (Fig. 2). Here, the major faults are identified as the Viscachaz, El Potro, Aranguiz and Mondaquita faults and the El Colorado and Mondaquita anticlines (Jensen, 1976) (Fig. 2 and 5). The faults correspond to west- and east-verging reverse faults that place the blocks of pre-rift basement over Mesozoic syn-rift successions and Upper Cretaceous-Cenozoic synorogenic deposits (Fig. 2). The faults have high angles at the surface, and the Mesozoic-Cenozoic deposits are frequently folded, buttressed and truncated against them (Figs. 5, 6 a and b ). The footwall faults frequently show west- and east-inclined panels that contain some subsidiary east-verging folds and thin-skinned thrusts (Figs. 2 and 5 c). The marine and continental syn-rift Jurassic deposits exposed on the footwall and hanging wall faults of the Vizcachas, Berracal and the south termination of the El Potro Fault (Figs. 2 and 6 b) suggest that this fault system could correspond to the partial inversion and reverse faulting of the Mesozoic basin edge (Martínez et al., 2016).

The basement-cored anticlines consist of asymmetrical east-verging folds composed of long and gently-dipping back limbs and short, steeply-dipping forelimbs (Figs. 2 and 5) involving Permo-Triassic granitic and volcanic rocks, Mesozoic syn-rift deposits and Cenozoic synorogenic successions (Figs. 2 and 5). Previous interpretations (Martínez et al., 2015) indicated that these structures could be explained by a thick-skinned imbricate system composed of east-verging ramps and west-verging backthrusts, associated with a generalized eastward motion of the orogenic belt at this latitude.

### 2.3. Preexisting evidence for late Cretaceous and Cenozoic deformation

The best evidence for Late Cretaceous to Cenozoic compressive deformation is well preserved in the Lagunillas Basin, along the Chacay

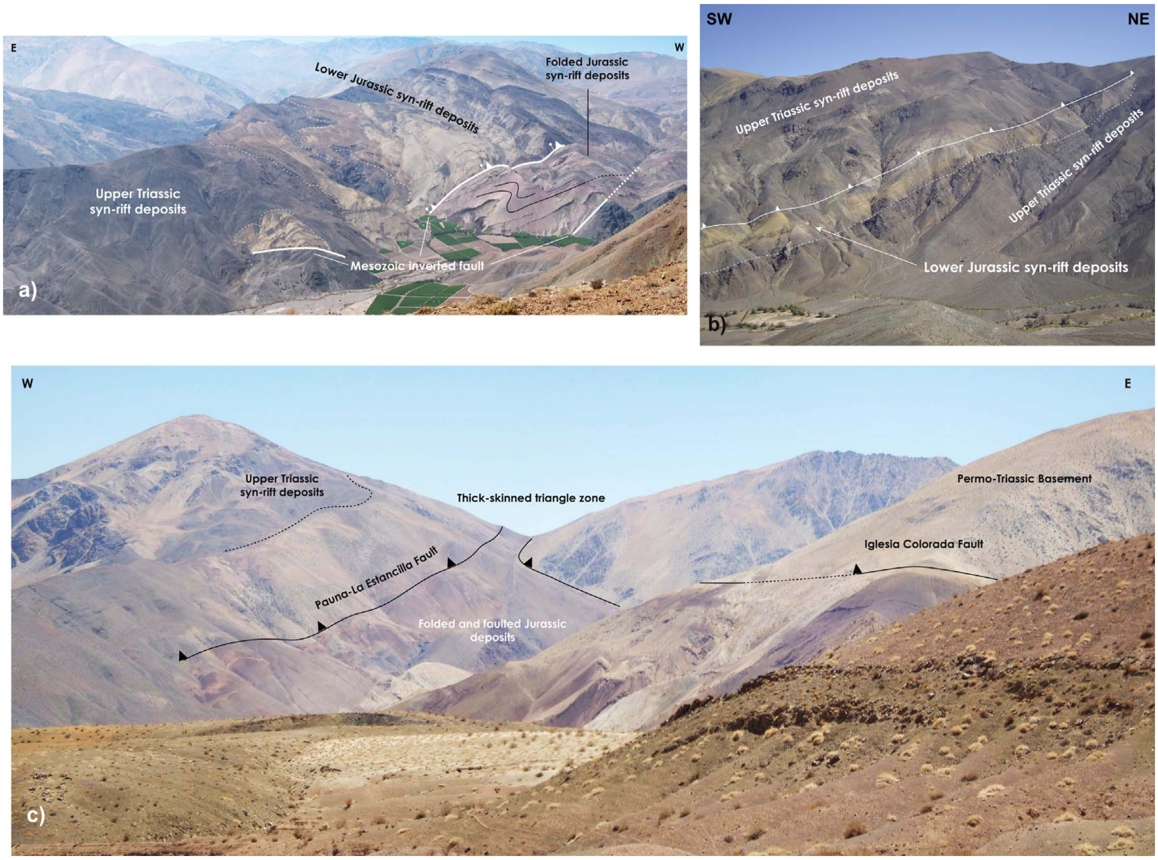


**Fig. 4.** (a) Mesozoic, inverted normal fault and the west-vergent inversion anticline exposed along the west edge of the Lautaro Basin, (b) oblique view and stratigraphic repetition of the Mesozoic successions along the east-vergent El Chancho Thrust in the Lautaro Basin, (c) Panoramic east-west view of the basement-involved faults (Pauna-La Estancilla and Iglesia Colorada faults) forming a thick-skinned triangle zone (See locations of the photos in Fig. 2).

River (Fig. 2). Here, the evidence consists of synorogenic deposits that unconformably cover the Triassic and Jurassic syn-rift successions and some intraformational unconformities (Fig. 5b and d). These deposits correspond to the Quebrada Seca Formation (see Section 2). They generally lie well exposed on the footwall of basement-involved reverse faults (e.g., Aranguiz and Mondaquita faults; Fig. 6a) and on the forelimbs of some footwall synclines (Figs. 2 and 5 b), and commonly contain a series of growth strata that record the tectonic activity of the faults and folds during their accumulation (Fig. 5b). The basal sections of the growth strata (basal red beds) are frequently more inclined, while the upper sections have lower dip angles (Fig. 5b) and generally shown onlap terminations. This situation is observed on the footwall of the Aranguiz and Mondaquita faults (Fig. 5d). In addition, some intraformational unconformities also have been recognized within the upper section of the Quebrada Seca Formation exposed on the footwall of the Aranguiz Fault (Fig. 5d) that also indicate that a synchronic and progressive rotation during its deposition.

Previous studies (Martínez et al., 2015) carried out in this basin also demonstrated the synorogenic character of the younger volcanic Miocene deposits of the Doña Ana Formation, exposed along the easternmost part of this basin. Moreover, the angular unconformity between the Doña Ana Formation and the Quebrada Seca Formation provide an excellent evidence to interpret at least two different episodes of compressive deformation. Recent studies (Martínez et al., 2015) have reported U-Pb ages to the Quebrada Seca Formation of ~80 Ma for its sedimentary basal section that lie in angular unconformity over the Mesozoic syn-rift fill of the Lagunillas Basin. These were determined to detrital zircons and correspond to the maximum permissible depositional age and possibly the age of its basal section. Based on this geochronology data and this angular unconformity important deformation episode is proposed to have occurred during Late Cretaceous times (nez et al., 2015, 2016; nez et al., 2015, 2016).

## 3. Methods

### 3.1. U-Pb-LA-ICPMS geochronology

In order to obtain and refined the ages of the synorogenic deposits of the Quebrada Seca Formation, in this study we have incorporated new data obtained by U-Pb-LA-ICPMS geochronology. This method was used to determine the zircon ages of this formation. The samples analyzed consist of volcanic (IC-02A; tuff) and sedimentary (IC-03; tuffaceous sandstone) rocks collected from the middle and upper sections of the Quebrada Seca Formation (Fig. 2). A series of zircons from these two new samples were prepared at the Geochronological Laboratory of the University of Chile using a Frantz magnetic separator and heavy liquid procedures. The selection of the zircons was made by hand with an optical microscope. The U-Pb dating of the samples was made at the LEI Laboratory of the Universidad Nacional Autónoma de México using a laser Excimer coupled to a Quadrupole Mass Spectometre (Thermo Xii), which is mainly used to obtain zircon ages (Solari et al., 2010). The laser ablation diameter was fixed at 34 µm. Mean ages of the volcanic and detrital zircons analyzed were determined using Isoplot software v.3.7 (Ludwing, 2008).

### 3.2. Apatite fission track (AFT) analyses

In order to constrain the cooling history related to exhumation of the basement blocks exposed in this region, we analyzed apatite fission tracks from five samples of Permo-Triassic granitic rocks, which were previously dated at ~245–250 Ma using the U-Pb method on zircons (nez et al., 2014, 2015; nez et al., 2014, 2015). Sample locations are

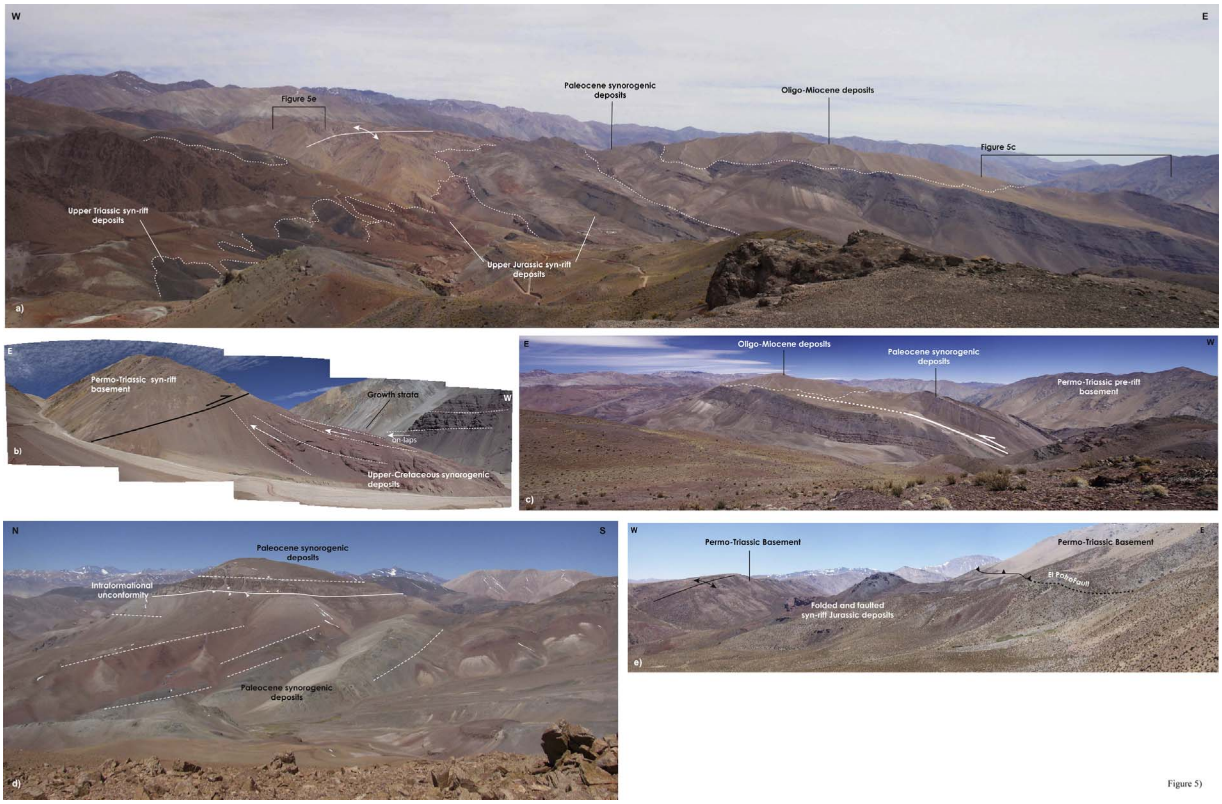


**Fig. 5.** (a) Core and back limb of the El Colorado Anticline along the central section of the Lagunillas Basin, (b) detail of the relationship between the Mondaquita Fault and the basal section of the Quebrada Seca Formation exposed on its footwall block. Note the onlaps termination in the growth strata, (c) subsidiary thin-skinned thrust involving the Paleocene synorogenic deposits of the Quebrada Seca Formation, (d) Aspect of the intra-formational unconformity observed within the upper section of the Quebrada Seca Formation exposed on the footwall of the Aranguiz Fault (See locations of the photos in Fig. 2).

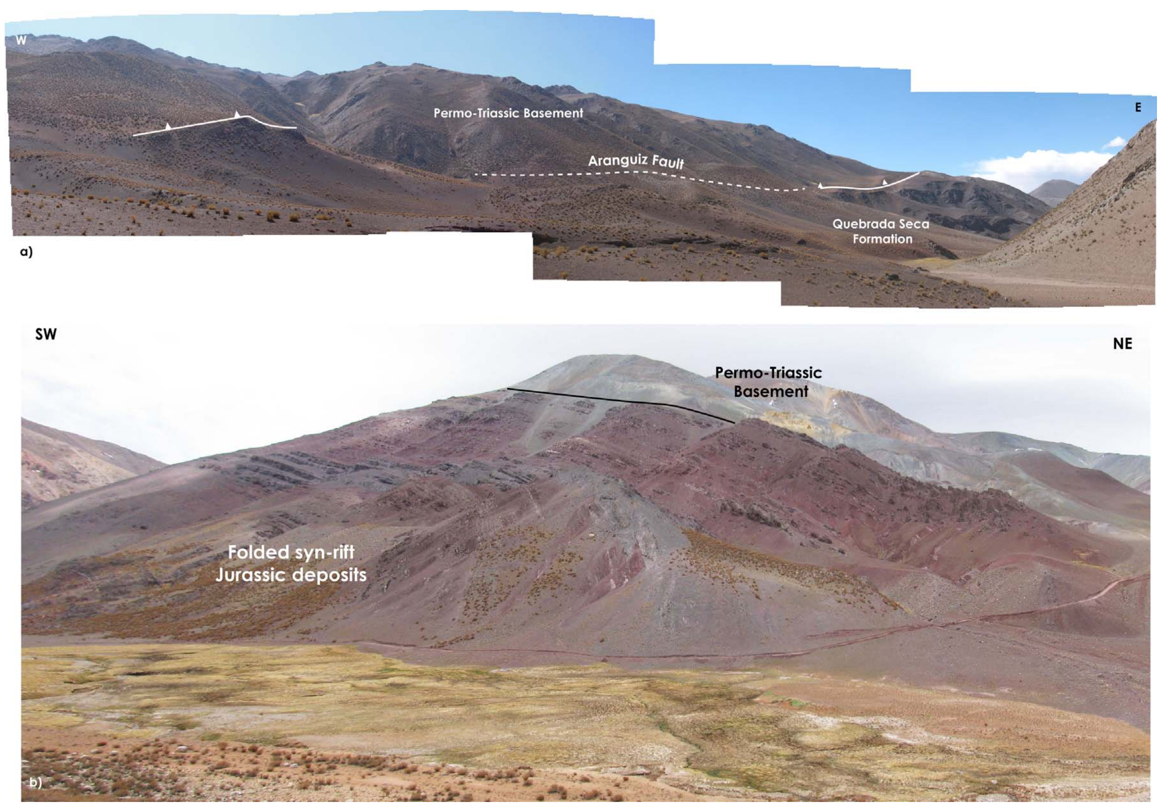


**Fig. 6.** (a) Panoramic view of the Aranguiz Fault, which place the Permo-Triassic Basement over the Paleocene synorogenic deposits of the Quebrada Seca Formation, (b) Aspect of the continental Jurassic syn-rift deposits of the Lagunillas Formation folded and buttressed against the Permo-Triassic Basement (See locations of the photos in Fig. 2).

**Table 1**
Apatite fission track ages. The notes under the table correspond to details of the method used here.

| Sample Number | Age of crystallization (U-Pb method) | Type | No. of Crystals | Elevation (m) | Track Density (×106 tracks cm$^{-2}$) (no. of tracks) | | | Mean Dpar (μm) | Age Dispersion (Pχ2) | Central Age (AFT method) (Ma) (± 1σ) | Apatite Mean Track Length (μm ± 1 s.e.) (no. of tracks) | Standard Deviation (μm) |
|---|---|---|---|---|---|---|---|---|---|---|---|---|
| | | | | | ρs (Ns) | ρi (Ni) | ρd (Nd) | | | | | |
| IC 58 | 256.8 ± 1.8 | Granite | 20 | 4100 | 0.4395 (191) | 1.694 (736) | 0.9458 (3027) | 2.72 | 0.01% (95.9%) | 45.0 ± 4.2 | 14.70 ± 0.22 (32) | 1.24 |
| IC 17 | 285.7 ± 2.0 | Monzonite | 20 | 1500 | 0.8281 (486) | 3.316 (1946) | 0.9322 (2983) | 2.44 | < 0.01 (> 99.9%) | 42.7 ± 2.9 | 14.28 ± 0.13 (100) | 1.25 |
| IC 22 | 253.3 ± 1.5 | Granodiorite | 20 | 3016 | 0.5831 (306) | 2.534 (1330) | 0.9168 (2939) | 2.06 | < 0.01 (99.7%) | 38.8 ± 3.0 | 14.11 ± 0.15 (100) | 1.49 |
| Bz | 258.5 ± 1.5 | Granite | 20 | 3635 | 0.6729 (388) | 2.116 (1220) | 0.9049 (2896) | 2.09 | < 0.01% (97.8%) | 52.8 ± 3.9 | 13.72 ± 0.21 (57) | 1.55 |
| BWD | 250 ± 2.1 | Granodiorite | 10 | 3014 | 0.7177 (418) | 2.115 (1232) | 0.8981 (2874) | 2.19 | < 0.01% (99.7%) | 55.8 ± 4.0 | 14.46 ± 0.12 (100) | 1.21 |

Notes:
(i). Analyses by external detector method using 0.5 for the 4π/2π geometry correction factor.
(ii). Ages calculated using dosimeter glass: IRMM540R with ζ540R = 368.1 ± 14.9 (apatite).
(iii). Pχ2 is the probability of obtaining a χ2 value for v degrees of freedom where v = no. of crystals − 1.
(iv). s.e. = standard error of the mean.

shown in Fig. 2. Apatite fission-track thermochronology is a technique commonly applied to interpret the cooling history and thermal history of rock units in the upper crust levels. This technique is used for estimating cooling ages between ~60 °C and 120 °C, an interval known as the "partial annealing zone" (PAZ) (Wagner and Reimer, 1972; Gallagher et al., 1998) and therefore allows determining the thermal history of the rocks at low temperatures, which commonly are used to constrain the time of exhumation of previously buried rock units. Fission-track length distribution gives information related to the velocity of the cooling history of the rocks along the PAZ.

Apatite grains were initially separated applying the same techniques used to separate zircons explained in Section 5.1. They were then prepared using standard procedures at the Fission-Track Laboratory of the Department of Geosciences of the University of Arizona (Table 1). Nearly 20 grains were analyzed from samples IC 58, IC 17, IC 22 and Bz. Only 10 grain were obtained for sample BWD (Table 1). The confined track lengths, the angle between the confined tracks, the c-crystallographic axis, and the kinetic parameter related to the figure length $D_{par}$were measured (Table 1). All samples passed the χ2 test (Galbraith, 2005), indicating that the distribution of counted fission tracks corresponds to a single population, which is consistent with a purely Poissonian variation (Galbraith, 2005). Thermal history modeling was performed using HeFTy (Ketcham, 2005), which considers AFT ages, track lengths and $D_{par}$ measurements allowing to determine time-temperature paths through inverse Monte Carlo modeling (10,000 inversions were run). The restrictions applied to the modeling are based on geological data, such as angular unconformities associated with Mesozoic syn-rift phases (Martínez et al., 2015), and the ages of synorogenic deposits shown here. To obtain a goodness-of-fit between modeled and measured track length distributions we used the Kolmogorov-Smirnov test with values of 0.5 and 0.05 for both, good and acceptable fits.

## 4. Results

### *4.1. U-Pb chronology of the Quebrada Seca formation*

The U-Pb analysis (U238/Pb206) of detrital zircons obtained from tuffaceous sedimentary rocks of the Quebrada Seca Formation reported a maximum depositional age of 66.0 ± 0.48 Ma (IC-03), while igneous zircons collected from the upper section reported a crystallization age of 60.2 ± 0.9 Ma (Fig. 2 and 7). The detrital zircons show three major populations of Permo-Triassic (240–290 Ma), Mesozoic (140–170 Ma) and Late Cretaceous (60–70 Ma) rocks (Fig. 7). The Late Cretaceous population was previously recognized by Martínez et al. (2015) in samples of the basal section of this formation, and it was considered as the maximum depositional age of this unit. Both ages reported here (IC-02A and IC-03) coincide partially with the ages determined by Iriarte et al. (1999) and Martínez et al. (2015) from synorogenic deposits located on the footwall of the Vizcachas and Aranguiz fault. Our new data are in agreement with the previous ages proposed for the Quebrada Seca Formation. Considering that in the study area this units show some stratigraphic features associated with synorogenic deposits, we only can interpret that this was accumulated under a contractional deformation regime during the Paleocene.

### *4.2. AFT constraints on exhumation and thermal modeling*

The basement-rock samples analyzed here were collected at 1500 and 4100 m a.s.l. (Table 1), and at the base and top of the granitic blocks, such as shown in Fig. 2. Sample BWD and Bz yielded an AFT ages of 55.8 ± 4.0 Ma and 52.8 ± 3.9 Ma (Table 1), corresponding to the oldest ages. Samples IC-17 and IC-58 yielded AFT ages of 42.7 ± 2.9 and 45.0 ± 4.2 Ma, respectively (Table 1) and sample IC-22 yielded an AFT age 33.8 ± 3 of Ma. As illustrated in Fig. 8, the mean track lengths of the samples analyzed range between 13.72 (Bz) and 14.70 μm (BWD, IC-17, IC 22, IC-58) (Table 1). The results of the

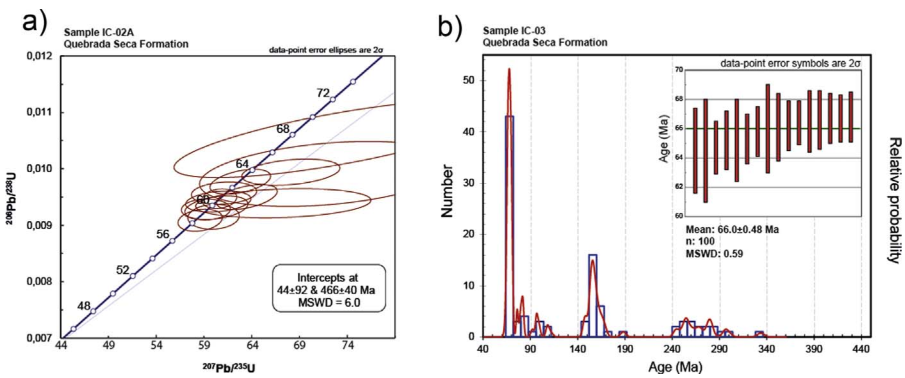


**Fig. 7.** (a) Concordia plots of LA-ICPMS U–Pb analysis of zircons from the sample IC-02 of the Quebrada Seca Formation, (b) Weighted mean age calculation for the U-Pb age of the sample IC-02 (c) Probability density plot and stacked histogram of detrital zircon U-Pb age and weighted mean age calculation for sedimentary rock of the Quebrada Seca Formation.

AFT ages and the mean track lengths (Fig. 8) indicate that a rapid cooling related to exhumation of the basement blocks occurred during the Late Paleocene and Eocene. According to Ring et al. (1999), the exhumation is mostly referred to "the unroofing history of a rock, defined by the vertical distance transverse by the rock relative to the Earth's surface" and this process can occur under different tectonic scenarios.

## 5. Discussion

### 5.1. Deformation sequence

The interpretation of the deformation sequence of orogenic systems that result from the tectonic inversion of inherited extensional faults could be difficult because the structural style in these regions is not commonly a thrust wedge and they are mostly dominated by basement-involved structures intercalated with some intramontane basins, similar to occur along the flat-slab subduction segment (28° − 29°S) of northern Chile. The combination of the new results obtained from this work joint others previously published (Salazar et al., 2013; Martínez et al., 2015; Rossel et al., 2016; Fig. 9) have allowed to understand how occurred the Andean deformation in the Frontal Cordillera of northern Chile from Late Cretaceous times. The results indicate that the tectonic structure of this region (Fig. 9) was developed during four important orogenic phases that have apparently occurred diachronically during different periods: Late Cretaceous, Paleocene, Eocene and Oligo-Miocene, however; we only show new data that mainly support the Paleocene and Eocene.

The chronological data (U-Pb ages) previously reported by Martínez et al. (2015) suggest that the Andean deformation in this region could be started as early as Late Cretaceous by the tectonic inversion of Jurassic half-grabens (Lautaro and Lagunillas basins), however; we have not new U-Pb ages that allow to confirm this interpretation. Nevertheless, our field observations coincide with this interpretation. Evidence of tectonic inversion of ancient Jurassic normal faults are observed along the Lautaro (to the east of the study area) and Lagunillas basins, where marine and continental syn-rift Jurassic and Triassic deposits are folded and strongly buttressed along reactivated Mesozoic basement faults (e.g., Mondaquita faults; Fig. 6b), many which could be hidden under younger reverse faults (E.g., Vizcachas Fault; Martínez et al., 2015). This confirms the idea that the Andean deformation in the Chilean Frontal Cordillera was initially controlled by the tectonic inversion of previous Mesozoic normal faults.

Similar structural styles have also been interpreted in another areas of the Central and Southern Andes (Chañarcillo and Salar de Atacama basins, Domeyko Range, Neuquén and Cuyo basins, San Jorge Gulf, among others), and many of them suggest that they have resulted from the positive reactivation of Mesozoic extensional systems during the Late Cretaceous creating the initial uplift of the orogenic belt (Mpodozis et al., 2005; Amilibia et al., 2008; Martínez et al., 2013; Peña et al., 2014; Folguera et al., 2015; Fennell et al., 2015; Rojas Vera et al., 2015; Bascuñan et al., 2015).

The new U-Pb ages reported in this work indicate that the Chilean Frontal Cordillera was affected by an orogenic episode that occurred during the Paleocene, possibly associated with the eastward advance of a basement-involved reverse faults (Vizcachas, Aranguiz faults; Fig. 2) affecting the pre-rift basement blocks of the Lagunillas Basin. This episode is mainly recorded by those volcanic and sedimentary synorogenic successions that occupy the footwall blocks of the basement-involved reverse faults (e.g., Quebrada Seca Formation; Martínez et al., 2015). This result allows changing a common interpretation about the contractional deformation of this sector of the Central Andes in this part of northern Chile, which was traditionally believed to have occurred during the Oligocene-Miocene (Godoy and Davidson, 1976; Jensen, 1976; Moscoso and Mpodozis, 1988, among others). Even, these results indicate that during the Paleocene this region was mostly shorted and not extended, such as it was argued by some workers (Cornejo et al., 2003).

Other important episode occurred during the Eocene, which is recorded by the new apatite fission track ages reported to the pre-rift basement blocks in this work (Figs. 2 and 7). This episode is associated with a rapid cooling related with exhumation. We interpreted that this cooling was accompanied of a progressive uplift of the basement reverse faults (Iglesia Colorada, Pauna-La Estancilla, Vizcachas, Aranguiz faults, among others) that have started during the Paleocene. These ages usually coincide with the age reported to the Incaic tectonic phase proposed by Steinman (1929) and broadly recognized in northern Chile. The Incaic tectonic phase in northern Chile was marked by an important contractional deformation, characterized by the eastward advance of basement-involved thrust systems (Coutand et al., 2001; Arriagada et al., 2016; Amilibia et al., 2008; Charrier et al., 2009; Martínez et al., 2016). The crustal shortening in this region provoked an important thickening of the continental margin and an accelerated uplift of the buried oldest rocks (Maksaev and Zentilli, 1999; Charrier et al., 2009). In the study region, this episode appears to be controlled by the propagation of large reverse faults and east- and west-verging ramps (Fig. 9; nez et al., 2015, 2016; nez et al., 2015, 2016) that initially uplifted the Permo-Triassic pre-rift basement blocks during the Paleocene. We suggest that the Eocene apatite fission track ages reported here, indicate that, possibly the crustal uplift related to reverse faulting was progressively accompanied of a rapid exhumation by erosion between 55 and 38 Ma.

Other similar exhumation ages related to erosion of basement blocks have been reported to some places of the Chilean Central Andes and nearby areas in northwestern Argentina and Bolivia (La Guradia, Domeyko Range, Eastern Cordillera, Salar de Atacama, Arizao Basin, Salar de Pastos Grandes, among others; Iriarte et al., 1999; Maksaev and Zentilli, 1999; Coutand et al., 2001; Barnes et al., 2007; Carrapa et al., 2009; Carrapa et al., 2011; DeCelles et al., 2011; Eichelberger and McQuarrie, 2015; Carrapa and DeCelles, 2015). Although we doñt observe an important angular unconformity between the deformed Paleocene and Eocene synorogenic deposits, other recent studies from

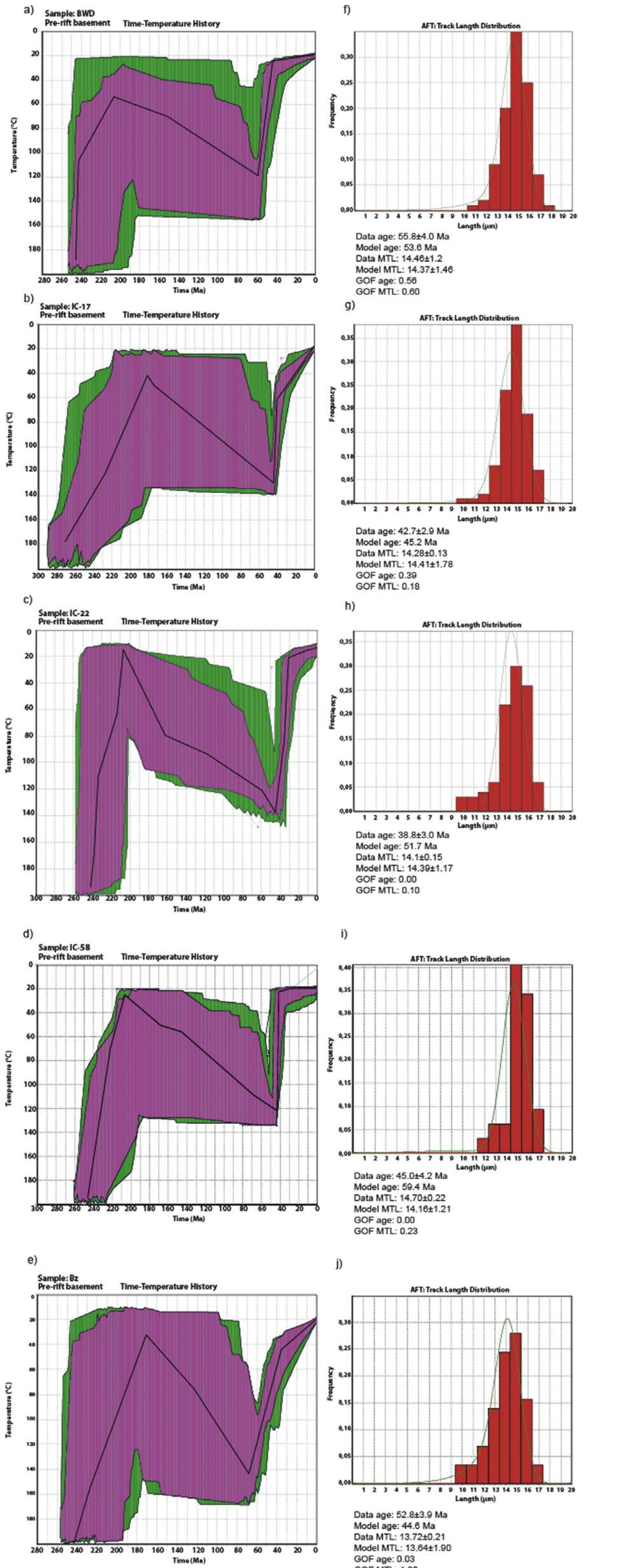


**Fig. 8.** (a–e) Time-temperature paths obtained from thermal history modeling using HeFTy software (Ketcham, 2005) for samples of the Permo-Triassic granitic rocks located in Fig. 2. The outer envelope contains acceptable fits, the inner shaded envelope contains good fits and thick black line indicates best fit model, (f–i) track length distribution histograms.

Rossel et al. (2016) carried out to the south of the Frontal Cordillera if have identified this unconformity, and also interpreted both Paleocene and Eocene deformation stages to this region. Some synorogenic deposits identified in northern Chile (Domeyko Range, Salar de Atacama Basin; Mpodozis et al., 2005; Arriagada et al., 2006; Bascuñan et al., 2015) has reported Eocene ages indicating thus, that this period was mostly dominated by crustal shortening. The AFT ages reported in this study, have allowed documenting the Incaic Orogeny in the Chilean Frontal Cordillera, which was unknown in the region for many years. Although the extensional tectonic is considered the most efficient mechanism to the exhumation of deep rocks, this mechanism does not work to the Frontal Cordillera where the structural framework is essentially compressive.

The thermal modeling of the apatite fission track ages (Fig. 8) shows similar solutions for the different basement blocks of the study area. Based on this, we can only posit for sure that part of the exhumation history includes Eocene cooling. We do not rule out that this region could have experienced a more complex exhumation history, however; a more detailed sampling is necessary to check it. On the other hand, the similarity between the thermal solutions determined here suggests that exhumation was partially synchronous in the different basement blocks.

Finally a last compressive episode is interpreted to have occurred during Miocene times, however; this is mostly constrained by the previous ages (mainly U-Pb and K-Ar) of the folded and synorogenic volcanic deposits of the Miocene Doña Ana Formation exposed along the triangle zone formed between the Aranguiz and Mondaquita reverse faults (Moscoso et al., 2010; Martínez et al., 2015) (Figs. 2 and 5 d). This event is associated with the final activity of both faults, which could have lasted until the Pliocene. Our field observation shows that this deposits unconformably overlies the Paleocene Quebrada Seca Formation in the easternmost part of the Lagunillas Basin (Fig. 2) and this angular unconformity mark the separation between two tectonic episodes. This event is better constrained in the Argentinean side (e.g., Sierra de Las Planchadas and the Sierra de Famatina, Sierra de Maz, Sierra de Urango) from the apatite fission track ages and analyses of synorogenic deposits (Coughlin et al., 1998; Dávila and Astini, 2007; Safipour et al., 2015, among others), indicating thus that deformation migrated toward the east of the study region and was concentrated mostly on the Argentinian side, creating a broken foreland setting. Recent studies (Zhou et al., 2017) also have documented an important Neogene deformation along some basins in the NW Argentinean that occurred at ca. 25–20 Ma by basement-involved thrust faults, possibly related to the reactivation of inherited structures and suggest that during the Eocene the major relief in the Central Andes was created on its western side. This Neogene contractional deformation is known as the "Quechua orogenic phase" (Mégard, 1984), which has traditionally been considered as the main responsible for the uplift of the Sierras Pampeanas in the eastern slope of the flat-slab segment of the Central Andes (Jordan et al., 1983; Ramos et al., 2002; Dávila and Astini, 2007; Dávila and Carter, 2013).

## 6. Conclusions

The structural configuration of the Frontal Cordillera in northern Chile is characterized by a mix of inverted and basement-involved compressive structures. In this region, the Andean deformation was initially controlled by the partial tectonic inversion of previous Mesozoic normal faults, which is mainly evidenced by the occurrence of inversion and basement-cored anticlines that affect the syn-rift deposits (Triassic and Jurassic) of the Lautaro and Lagunillas basins. This episode appears to have occurred in the Late Cretaceous and suggests that the pre-orogenic configuration played an important role in the initial deformation of this region. The following Andean deformation was controlled by basement-involved reverse faults during the Paleocene-Eocene and Miocene times, creating thus the complete configuration of this part of the Central Andes. The U-Pb ages of the synorogenic deposits reported here indicate an eastward migration of the deformation, while the AFT ages show that a rapid cooling of the basement blocks

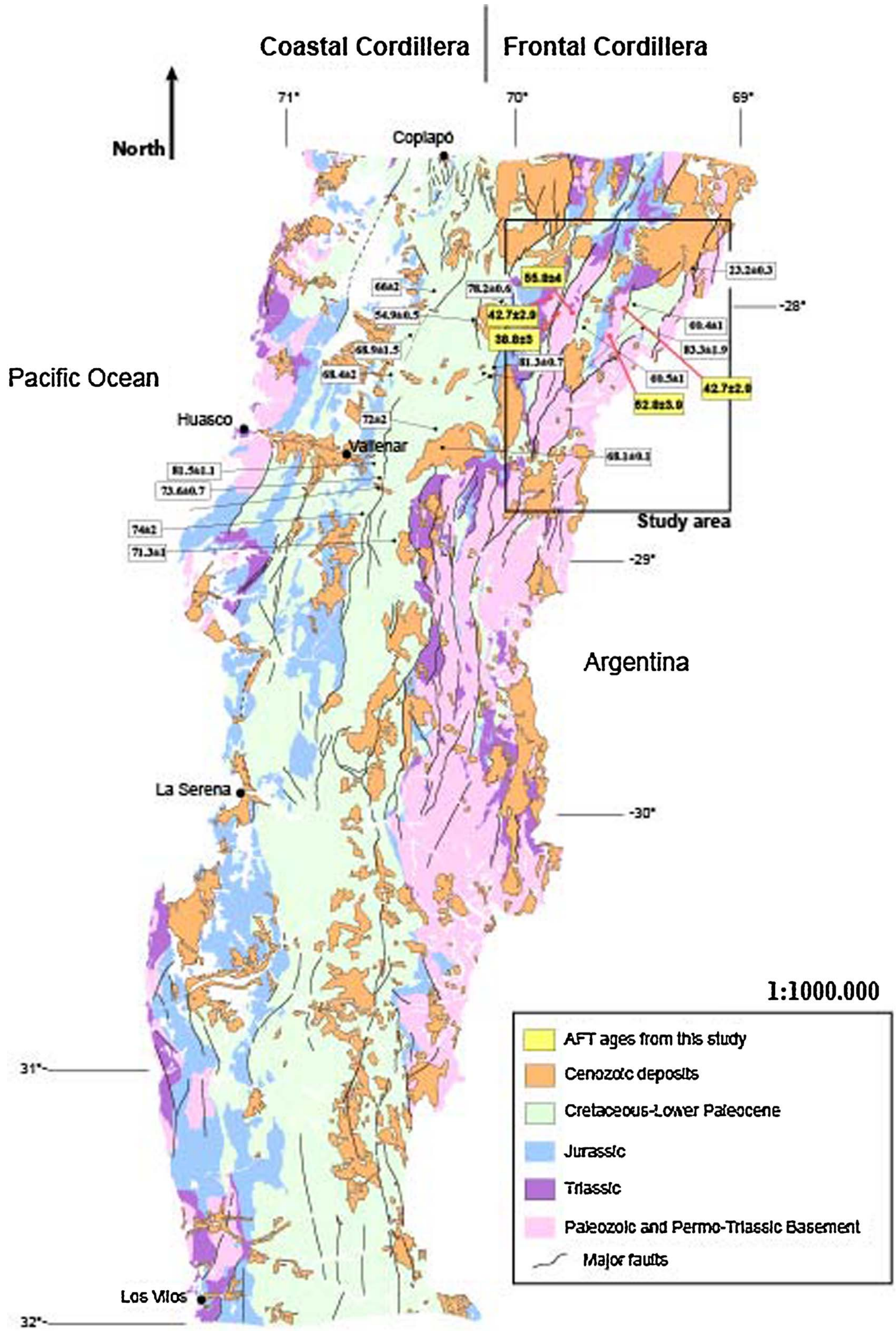


**Fig. 9.** Simplified geological map of the northern Chile between 28°–32°S, showing the distribution of the U-Pb and K-Ar ages from synorogenic deposits obtained by previous studies (black numbers) (Arévalo, 2005b; Arévalo and Welkner, 2008; Maksaev et al., 2009; Moscoso et al., 2010; Arriagada et al., 2013; Rodríguez, 2013), as well as the distribution of the new AFT ages determined from this study.

occurred during Eocene times. Our U-Pb and AFT data also correlate well with the major orogenic phases (Peruvian, Incaic and Quechua) identified in neighboring provinces along the Central Andes, which sometimes are separated by extensional episodes. Here, however, we interpreted tha the Incaic tectonic phase is the most important tectonic phase responsible for basement deformation and uplift in the Chilean Frontal Cordillera. The pattern of AFT thermal solutions for the Permo-Triassic granitic rocks indicates a coeval exhumation of different tectonic blocks. This situation may be related to synchronous basement thrusts motion during the Eocene.

## Acknowledgments

This work has been supported by the research project "The crustal structure and timing of deformation along the Chilean flat-slab subduction segment (27°–29°S), Central Andes", funded by the Fondo Nacional de Desarrollo Científico y Tecnológico (Fondecyt), Chile (grant 3140557). The authors thank the fruitful discussion with Dr. Constantino Mpodozis on different aspects related to the regional geology of the study area, as well as and the earliest reviewed of Dr. Federico Dávila. On the other hand, we thank Midland Valley Company for the academic license for the Move software, which was used for the structural modeling. Also, we would like to thank J. Vargas and R. Valles (Geology Department, Universidad de Chile), for zircon sample preparation, as well as L. Solari for the U–Pb LA-ICP-MS analyses (LEI, UNAM). Finally we thank the comments of two anonymous reviewers that help to improve the early version of this manuscript.

## References

Amilibia, A., Sàbat, F., McClay, K.R., Muñoz, J.A., Roca, E., Chong, G., 2008. The role of inherited tectono-sedimentary architecture in the development of the central Andean mountain belt: insights from the Cordillera de Domeyko. J. Struct. Geol. 30, 1520–1539.
Arévalo, C., Welkner, D., 2008. Carta Carrizal Bajo-Chacritas, Región de Atacama, Carta Geológica Básica. Servicio Nacional de Geología y Minería, Santiago scale: 1:100.000.
Arévalo, C., 2005. Carta los Loros, Región de Atacama, Carta Geológica Básica, vol. 92 Servicio Nacional de Geología y Minería, Santiago 54 p, scale: 1:100.000.
Arriagada, C., Ferrando, R., Córdova, L., Morata, D., Roperch, P., 2013. The Maipo Orocline: a firts scale structural feature in the Miocene to recent geodynamic evolution in the central Chilean Andes. Andean Geol. 4 (3), 419–437.
Baraganzi, M., Isacks, B.L., 1976. Spatial distribution of earthquakes and subduction of theNazca plate beneath South America. Geology 4, 686–692.
Barnes, J.B., Ehlers, T.A., McQuarrie, N., ÓSullivan, P.B., Pelletier, J.D., 2007. Eocene to recent variations in erosion across the central Andean fold thrust belt, northern Bolivia: implications for plateau evolution. Earth Planet. Sci. Lett. 248, 118–133.
Bascuñan, S., Arriagada, C., Le Roux, J., Deckart, K., 2015. Unraveling the Peruvian phase of the Central Andes: stratigraphy, sedimentology and geochronology of the Salar de Atacama Basin (22°30–23°S), northern Chile. Basin Res. http://dx.doi.org/10.1111/bre.12114.
Carrapa, B., DeCelles, P.G., 2015. Regional exhumation and kinematic history of the central Andes in response to cyclical orogenic processes. In: DeCelles, P.G., Ducea, M.N., Carrapa, B., Kapp, P.A. (Eds.), Geodynamics of a Cordilleran Orogenic System: The Central Andes of Argentina and Northern Chile, memoir 212. Geological Society of America, pp. 201–213.
Carrapa, B., Schoenbhom, L., DeCelles, P.G., Clementz, M., Hungtington, K., 2009. Surface response to lithospheric delamination: an example from the Puna Plateau of NW Argentina. Geol. Soc. Am. Abstr. Prog.. 41, 516.
Carrapa, B., Trimble, J., Stockli, D., 2011. Patterns and timing of exhumation and deformation in the Eastern Cordillera of NW Argentina revealed by (U-Th)/He thermochronology. Tectonics 30. http://dx.doi.org/10.1029/2010TC002707.
Charrier, R., 1979. El Triásico en Chile y regiones adyacentes de Argentina: Una reconstrucción paleogeográfica y paleoclimática. Comunicaciones 26, 1–47.
Charrier, R., Farías, M., Maksaev, V., 2009. Evolución tectónica, paleogeográfica y metalogénica durante el Cenozoico en los Andes de Chile norte y central e implicancias para las regiones adyacentes de Bolivia y Argentina. Rev. Asoc. Geol. Arg. 65, 5–35.
Cornejo, P., Mattews, S., Pérez De Arce, C., 2003. The K-T compressive deformation event in northern Chile (24°–27°S). Paper Presented at X Congreso Geológico Chileno, Concepción.
Coughlin, T.J., O'Sullivan, P.B., Kohn, B., Holcombe, R.J., 1998. Apatite fission-track thermochronology of the Sierras Pampeanas, central western Argentina: implications for the mechanism of plateau uplift in the Andes. Geology 26, 999–1002.
Coutand, I., Cobbold, P.R., de Urreiztieta, M., Gautier, P., Chauvin, A., Gapais, D., Rossello, E.A., Lòpez-Gamundí, O., 2001. Style and history of andean deformation, puna plateau, northwestern Argentina. Tectonics 20, 210–234.
Cristallini, E., Cominguez, A.H., Ramos, V.A., Mercerat, E., 2004. In: In: McClay, K.R. (Ed.), Basement Double Wedge Thrusting in the Northern Sierras Pampeanas of Argentina (27°S). Constrain from Deep Seismic Reflection, vol. 82. Thrust Tectonics and Hydrocarbon Systems, pp. 65–90 AAPG Memoir.
Dávila, F., Astini, R., 2007. Cenozoic provenance history of synorogenic conglomerates in western Argentina (Famatina belt): Implications for Central Andean foreland development. Geol. Soc. Am. Bull. 119, 609–622. http://dx.doi.org/10.1130/B26007.1.
Dávila, F., Carter, A., 2013. Exhumation history of the Andean broken foreland revisited. Geology 41, 443–446.
DeCelles, P.G., Carrapa, B., Horton, B., Gehrels, G., 2011. Cenozoic foreland basin system in the central Andes of northwestern Argentina: implications for Andean geodynamics and modes of deformation. Tectonics 30, TC6013. http://dx.doi.org/10.1029/2011TC002948.
Eichelberger, N., McQuarrie, N., 2015. Kinematic reconstruction of the Bolivian orocline. Geosphere 11. http://dx.doi.org/10.1130/ges01064.1.
Fennell, L., Folguera, A., Naipauer, M., Gianni, G., Rojas Vera, E., Bottesi, G., Ramos, V., 2015. Cretaceous deformation of the southern Central Andes: synorogenic growth strata in the Neuquén Group (35°30′–37°S). Basin Res. 1–22. http://dx.doi.org/10.1111/bre.12135.
Folguera, A., Bottesi, G., Duddy, I., Martín-Gonzalez Orts, D., Sagripanti, L., Vera Rojas Ramos, V.A., 2015. Exhumation of the Neuquén Basin in southern Central Andes (Malargüe fold and thrust belt) from field data and low-temperature thermochronology. J. South Am. Earth Sci. 64, 381–398.
Galbraith, R., 2005. Statistics for Fission Track Analysis: Interdisciplinary Statistics, 1st ed. Chapman & Hall/CRC, Boca Raton, Florida.
Gallagher, K., Brown, R., Johnson, C., 1998. Fission track analysis and its applications to geological problems. Ann. Rev. Earth Planet. Sci. 26, 519–572.
Godoy, E., Davidson, J.D., 1976. Pilares en compresión de edad Mioceno superior en los Andes del Norte de Chile (22°–30°Latitud Sur). Paper Presented at I Congreso Geológico Chileno, vol. 1, 87–103.
Gregori, D.A., Greco, L.E., Llambías, E., 2003. El intrusivo López Lecube: evidencias de magmatismo alcalino Gondwánico en el sector sudoeste de la provincia de Buenos Aires, Argentina. Rev. Asoc. Geol. Arg. 58, 176–186.
Gutscher, M.A., Spakman, W., Bijwaard, H., Engdahl, E.R., 2000. Geodynamic of flat subduction: seismicity and tomographic constraints from the Andean margin. Tectonics 19, 814–833.
Hervé, F., Fanning, M., Calderón, M., Mpodozis, C., 2014. Early permian to late triassic batholiths of the chilean frontal cordillera (28°–31°S): SHRIMP U–Pb zircon ages and Lu–Hf and O isotope systematics. Lithos 184–187, 436–446.
Iriarte, S., Arévalo, A., Mpodozis, C., 1999. Hoja La Guardia, Región de Atacama. Servicio Nacional de Geología y Minería, Santiago scale 1:100.000.
Jensen, O., 1976. Geología de las nacientes del río Copiapó, entre los 27°53′ y 28°20′ de latitud Sur, provincia de Atacama. Memoria de Titulo (Inédito). Universidad de Chile, Departamento de Geología, Chile 249 pp.
Jordan, T., Isacks, B.L., Allmendinger, R., Brewer, J., Ramos, V.A., Ando, C., 1983. Andeantectonics related to geometry of subducted Nazca plate. Geol. Soc. Am. Bull. 94, 341–361.
Ketcham, R., 2005. Forward and inverse modeling of low-temperature thermochronometry data. Rev. Mineral. Geochem. 58, 275–314.
Ludwing, K.R., 2008. Isoplot 3.6.4, special, publication. Berkley Geochronology Center.
Mégard, F., 1984. The Andean orogenic period and its major structures in central and northern Peru. J. Geol. Soc. Lond. 141, 893–900.
Maksaev, V., Zentilli, M., 1999. Fission track thermochronology of the Domeyko Cordillera, northern Chile; implications for Andean tectonics and porphyry copper metallogenesis. Explor. Min. Geol. 8, 65–89.
Maksaev, V., Munizaga, F., Valencia, V., Barra, F., 2009. LA-ICP-MS zircón U-Pb geochronology to constrain the age of post-Neocomian continental deposits of the Cerrillos Formation, Atacama Region, northern Chile: tectonic and metallogenic implications. Andean Geol. 36, 264–287.
Martínez, F., Arriagada, C., Mpodozis, C., Peña, M., 2012. The Lautaro Basin: a record of inversion tectonics in northern Chile. Andean Geol. 39 (2), 258–278.
Martínez, F., Arriagada, C., Peña, M., 2014. Mapa geológico Iglesia Colorada-Cerro del Potro y Cerro de Mondaquita, Región de Atacama. Geología Básica. Servicio Nacional de Geología y Minería, Santiago, Chile.
Martínez, F., Arriagada, C., Valdivia, R., Deckart, K., Peña, M., 2015. Geometry and kinematics of the Andean thick-skinned thrust systems: insights from the Chilean Frontal Cordillera (28°–28.5°S), Central Andes. J. South Am. Earth Sci. 64, 307–324.
Martínez, F., Arriagada, C., Peña, M., Deckart, K., Charrier, R., 2016. Tectonic styles and crustal shortening of the Central Andes Pampean flat-slab segment in northern Chile (27°–29°S). Tectonophysics 667, 144–162.
Moscoso, R., Mpodozis, C., 1988. Estilos estructurales en el Norte Chico de Chile (28°–31°S), regiones de Atacama y Coquimbo. Rev. Geol. Chile 15, 155–158.
Moscoso, R., Mpodozis, C., Nassi, C., Ribba, L., (Compilador) Arévalo, C., 2010. Geología de la Hoja El Tránsito, Región de Atacama. Servicio Nacional de Geología y Minería de Chile Serie Preliminar, 7, scale: 1:250.000, 3 anexos, Santiago.
Mpodozis, C., Kay, S., 1990. Provincias magmáticas ácidas y evolución tectónica deGondwana: Andes chilenos (28–31°S). Rev. Geol. Chile 17, 153–180.
Mpodozis, C., Ramos, V.A., 1989. The andes of Chile and Argentina. In: Ericksen, G.E., Cañas Pinochet, M.T., Reinemud, J.A. (Eds.), Geology of the Andes and Its Relation to Hydrocarbon and Mineral Resources, earth sciences series 11. Circumpacific Council for Energy and Mineral Resources, pp. 59–90.
Mpodozis, C., Ramos, V.A., 2008. Tectónica jurásica en Argentina y Chile: Extensión, Subducción Oblicua, Rifting, Deriva y Colisiones? Rev. Geol. Argent. 63, 479–495.
Muzzio, G., 1980. Geología de la región comprendida entre el Cordón de Varillar y Sierra Las Vizcachas, Precordillera de Copiapó, Chile. Memoria de Titulo (Inédito). Universidad de Chile, Departamento de Geología 176p.
Oliveros, V., Labbé, M., Rossel, P., Charrier, R., Encinas, A., 2012. Late Jurassic paleogeographic evolution of the Andean back-arc basin: new constrains from the Lagunillas gormation, northern Chile (27°30′–28°30′S). J. South Am. Earth Sci. 37, 25–40.
Peña, M., Arriagada, C., Martínez, F., Becerra, J., 2013. Carta Geológica Yerbas Buenas-Tres Morros, Región de Atacama. Servicio Nacional de Geología y Minería, Santiago scale:1:100.000.
Ramos, V.A., Folguera, A., 2009. Andean flat-slab subduction through time. In: Murphy, J.B., Keppie, J.D., Hynes, A.J. (Eds.), Ancient Orogens and Modern Analogues, special publication, 327. The Geological Society of London, pp. 31–54.
Ramos, V.A., Cristallini, E.O., Pérez, D.J., 2002. The pampean flat-slab of the central

andes. J. South Am. Earth Sci. 15, 59–78.
Ramos, V.A., 2009. Anatomy and global context of the Andes: main geologic features and the Andean orogenic cycle. In: Kay, S.M., Ramos, V.A., Dickinson, W.R. (Eds.), Backbone of the Americas: Shallow Subduction, Plateau Uplift, and Ridge and Terrane Collision, memoir 204. The Geological Society of America, pp. 31–65.
Ramos, V., 2010. The tectonic regime along the Andes: present day and Mesozoic regimes. Geol. J. 45, 2–25.
Reutter, K.J., 1974. Entwicklung und Bauplan der chilenischen Hochkordillere im Bereich 29º südlicher Breite. Neues Jahrbuch für Geologie und Paläontologie 146 (2), 153–178.
Ring, U., Brandon, M.T., Willet, S.D., Lister, G.S., 1999. Exhumation process. In: Ring, U., Brandon, M.T., Lister, G.S., Willett, S.D. (Eds.), Exhumation Process: Normal Faulting, Ductile Flow and Erosion, special publications, 154. Geological Society London, pp. 1–27.
Rodríguez, M.P., 2013. Cenozoic Uplift and Exhumation Above the Southern Part of the Flat Slab Subduction Segment of Chile (28.5–32°S). Unpublished Ph.D. Thesis. University of Chile, Santiago 181 p.
Rojas Vera, E., Mescua, J., Folguera, A., Becker, T.P., Sagripanti, L., Fennell, L., Orts, D., Ramos, V.A., 2015. Evolution of the Chos Malal and Agrio fold and thrust belts, Andes of Neuquén: insight from structural analysis and apatite fission track dating. J. South Am. Earth Sci. 64, 418–433.
Rossel, K., Aguilar, G., Salazar, E., Martinod, J., Carretier, S., Pinto, L., Cabré, A., 2016. Chronology of Chilean Frontal Cordillera building from geochronological, stratigraphic and geomorphological data insights from Miocene intramontane-basin deposits. Basin Res. http://dx.doi.org/10.1111/bre.12221.
Safipour, R., Carrapa, C., DeCelles, P.G., Thomson, S.N., 2015. Exhumation of the Precordillera and northern Sierras Pampeanas and along-strike correlation of the Andean orogenic front, northwestern Argentina. In: DeCelles, P.G., Ducea, M.N., Carrapa, B., Kapp, P.A. (Eds.), Geodynamics of a Cordilleran Orogenic System: The Central Andes of Argentina and Northern Chile. Geological Society of America Memoir, pp. 212. http://dx.doi.org/10.1130/2015.1212(10).
Salazar, E., Coloma, F., Creixell, C., 2013. Carta Geológica El Tránsito-Lagunillas, Región de Atacama. Servicio Nacional de Geología y Minería, Santiago scale:1:100.000.
Solari, L.A., Gómez-Tuena, A., Bernal, J.P., Pérez-Arvizu, O., Tanner, M., 2010. U–Pb zircón geochronology by an integrated LAICPMS micro analytical workstation: achievements in precision and accuracy. Geostand. Geoanal. Res. 34 (1), 5–18.
Steinman, G., 1929. Geologie von Peru. Carl Winters Universitats, Buchhandlung 448 pp.
Wagner, G.A., Reimer, G.M., 1972. Fission track tectonics: the tectonic interpretation of fission track ages. Earth Planet. Sci. Lett. 14, 263–268.
Zapata, T., Allmendinger, R., 1996. Thrust–front zone of the Precordillera, Argentina; a thick-skinned triangle zone. AAPG Bull. 80, 359–381.
Zhou, R., Schoenbohm, L., Sobel, E., Davis, D., 2017. New constraints on orogenic models of the southern Central Andean Plateau: Cenozoic basin evolution and bedrock exhumation. Geol. Soc. Bull. 129, 152–170.